

Imaging Atherosclerotic Plaque Inflammation With [¹⁸F]-Fluorodeoxyglucose Positron Emission Tomography

J.H.F. Rudd, MD, MRCP; E.A. Warburton, MD, DM; T.D. Fryer, PhD; H.A. Jones, PhD; J.C. Clark, DSc; N. Antoun, MD, FRCP, FRCR; P. Johnström, PhD; A.P. Davenport, PhD; P.J. Kirkpatrick, MSc, FRCS; B.N. Arch, PhD; J.D. Pickard, MD, FRCS; P.L. Weissberg, MD, FRCP

Background—Atherosclerotic plaque rupture is usually a consequence of inflammatory cell activity within the plaque. Current imaging techniques provide anatomic data but no indication of plaque inflammation. The glucose analogue [¹⁸F]-fluorodeoxyglucose (¹⁸FDG) can be used to image inflammatory cell activity non-invasively by PET. In this study we tested whether ¹⁸FDG-PET imaging can identify inflammation within carotid artery atherosclerotic plaques.

Methods and Results—Eight patients with symptomatic carotid atherosclerosis were imaged using ¹⁸FDG-PET and co-registered CT. Symptomatic carotid plaques were visible in ¹⁸FDG-PET images acquired 3 hours post-¹⁸FDG injection. The estimated net ¹⁸FDG accumulation rate (plaque/integral plasma) in symptomatic lesions was 27% higher than in contralateral asymptomatic lesions. There was no measurable ¹⁸FDG uptake into normal carotid arteries. Autoradiography of excised plaques confirmed accumulation of deoxyglucose in macrophage-rich areas of the plaque.

Conclusions—This study demonstrates that atherosclerotic plaque inflammation can be imaged with ¹⁸FDG-PET, and that symptomatic, unstable plaques accumulate more ¹⁸FDG than asymptomatic lesions. (*Circulation*. 2002;105:2708-2711.)

Key Words: atherosclerosis ■ imaging ■ nuclear medicine

Inflammation is important in both the pathogenesis and outcome of atherosclerosis.¹ Plaques containing numerous inflammatory cells, in particular macrophages, have a high risk of rupture, whereas those with few inflammatory cells are at lower risk.^{2,3} The current “gold standard” imaging technique for atherosclerosis is x-ray contrast angiography, which provides high-resolution definition of the site and severity of luminal stenoses, but no information about plaque inflammation.

There is a need to quantify plaque inflammation to predict the risk of plaque rupture and to monitor the effects of atheroma-modifying therapies. This is important because recent experimental and clinical studies strongly suggest that hepatic hydroxymethyl glutaryl coenzyme A reductase inhibitors (statins) promote plaque stability by decreasing plaque macrophage content and activity without substantially reducing plaque size and therefore angiographic appearance.⁴

[¹⁸F]-fluorodeoxyglucose (¹⁸FDG) is a glucose analogue that is taken up by cells in proportion to their metabolic activity.⁵ We tested the hypothesis that plaque inflammation could be visualized and quantified non-invasively using ¹⁸FDG-PET in patients with symptomatic carotid artery disease.

Methods

Patient Recruitment

We recruited 8 patients who had experienced a recent carotid-territory transient ischemic attack and had an internal carotid artery stenosis of at least 70%. Patients were excluded if they had either carotid artery occlusion or diabetes. The study protocol was approved by the local ethics committee and the UK Administration of Radioactive Substances Advisory Committee. All patients gave written informed consent.

PET Protocol

PET was carried out using a GE Advance PET scanner (GE Medical Systems). We administered 370 MBq ¹⁸FDG intravenously over 60 seconds. PET images (as 4×5 minute frames) were acquired in 3D mode, at 190 (±6) minutes after ¹⁸FDG administration. This time-point was chosen after preliminary dynamic studies indicated that late imaging provided optimal contrast between the ¹⁸FDG concentration in plaque and the main background region, namely blood.

A stiff cervical collar was worn to minimize patient movement. PET images were reconstructed using the 3D reprojection algorithm,⁶ with corrections applied for attenuation, dead time, scatter, and random coincidences. Rigid body co-registration with CT was performed, using a combination of fiducial markers and internal anatomical landmarks (spinal cord and muscles of the jaw and neck). This resulted in co-registration typically to within 1 mm in each dimension around the stenosis. To estimate plaque ¹⁸FDG concentration, three-dimensional volumes of interest (VOI) were drawn

Received March 5, 2002; revision received April 19, 2002; accepted April 22, 2002.

From the Division of Cardiovascular Medicine (J.H.F.R., H.A.J., P.L.W.), Division of Stroke Medicine (E.A.W.), Wolfson Brain Imaging Centre (T.D.F., J.C.C., J.D.P.), Department of Radiology (N.A.), Clinical Pharmacology Unit (P.J., A.P.D.), Division of Neurosurgery (P.J.K.), and Centre for Applied Medical Statistics (B.N.A.), University of Cambridge, Addenbrooke's Hospital, Cambridge, UK.

Correspondence to Professor Peter L Weissberg, Box 110, Level 6, ACCI, Addenbrooke's Hospital, Hills Road, Cambridge CB2 2QQ, UK. E-mail plw@mole.bio.cam.ac.uk

© 2002 American Heart Association, Inc.

Circulation is available at <http://www.circulationaha.org>

DOI: 10.1161/01.CIR.0000020548.60110.76

Details of Patients Who Underwent ¹⁸F-DG-PET Imaging

Patient	Sex	Age	Symptoms	Net ¹⁸ F-DG Accumulation Rate ($\times 10^{-5}$ sec ⁻¹) (Symptomatic)	Net ¹⁸ F-DG Accumulation Rate ($\times 10^{-5}$ sec ⁻¹) (Asymptomatic)
1	M	66	R amaurosis $\times 2$	5.88	3.44
2	M	71	Aphasia $\times 3$	8.05	—
3	F	48	R hemiparesis	7.59	4.95
4	M	68	L amaurosis $\times 2$	8.44	7.71
5	M	52	L hemiparesis $\times 6$	8.38	4.74
6	M	63	L hemiparesis $\times 2$	5.77	—
7	F	69	L hemisensory	10.87	9.91
8	M	71	R hemiparesis	8.65	6.49
	Female (%)	Mean age		Mean (SEM)	Mean (SEM)
	25	63.5		7.95 (± 0.58)	6.21 (± 0.96)

The values in the "Symptomatic" and "Asymptomatic" columns are the net ¹⁸F-DG accumulation rates for symptomatic and asymptomatic plaques, respectively. The absent values in the asymptomatic column represent patients with angiographically normal arteries on the asymptomatic side, in whom there was no significant accumulation of ¹⁸F-DG compared to background plasma. The bottom row of the table summarises the overall findings.

M indicates male; F, female; R, right; and L, left.

around the area of stenosis on the contrast CT scan using the Analyze software package (AnalyzeDirect).⁷ These regions were then placed onto the co-registered PET images to produce mean ¹⁸F-DG concentration values (kBq/mL). The mean VOI size was 148 mm³. To determine the plasma ¹⁸F-DG concentration up to the scan time (input function), venous blood was sampled throughout the PET study. The estimated net ¹⁸F-DG accumulation rate was determined by dividing the mean decay-corrected plaque VOI ¹⁸F-DG concentration by the integral of the decay-corrected input function, and is expressed in units of sec⁻¹.

CT Protocol

Using a GE Hispeed Advantage CT scanner (GE Medical Systems), helical contrast CT angiograms were acquired from skull base to 3 cm below the level of the carotid bifurcation.

Plaque Histology

After imaging, carotid endarterectomy samples from all 8 patients imaged were fixed and stained with hematoxylin and eosin. Immunohistochemistry was performed using anti-macrophage antibodies (CD68, Dako, Elys, UK).

Plaque Autoradiography

In a separate autoradiographic study, 3 carotid plaques from symptomatic patients were incubated whole with 50 μ Ci tritiated deoxyglucose (an in vitro analogue of ¹⁸F-DG) in 5 mL Medium 199 (Sigma) for 60 minutes at 37° C. Paraffin sections of 5 μ m thickness were coated with autoradiographic emulsion (LM-1, Amersham), exposed for 6 weeks, developed, and counterstained with hematoxylin and eosin. Control slides were prepared without radioactivity.

Statistical Methods

Results are expressed as mean \pm SEM with 95% CI in brackets. The paired *t* test was used to compare net ¹⁸F-DG accumulation rates in symptomatic and asymptomatic carotid plaques in the same patients.

Results

We performed ¹⁸F-DG-PET and CT scanning in 8 patients between 48 and 71 years of age (Table). The median time

between symptoms and PET study was 3.5 months, and between PET and carotid endarterectomy was 43 days. In all patients, co-registered PET images acquired around 3 hours revealed ¹⁸F-DG accumulation at the site of the symptomatic plaque (Figure 1).

Six of the 8 patients had contralateral asymptomatic stenoses ranging from 35% to 75%. A comparison was made between the net ¹⁸F-DG accumulation rate in symptomatic plaques and contralateral asymptomatic lesions. In all cases, symptomatic lesions had higher estimated ¹⁸F-DG accumulation rates than asymptomatic lesions; the mean symptomatic net accumulation rate was $7.95 \times 10^{-5} \pm 0.58 \times 10^{-5}$ sec⁻¹ (95% CI: 6.58 to 9.32×10^{-5}), with a mean difference between symptomatic and asymptomatic of $2.10 \times 10^{-5} \pm 0.45 \times 10^{-5}$ sec⁻¹ (95% CI 0.94 to 3.26×10^{-5} , $P=0.005$).

The 2 remaining patients had angiographically normal arteries on the asymptomatic side, with no significant uptake of ¹⁸F-DG into those vessels; the ¹⁸F-DG concentration in a VOI around the carotid bifurcation did not differ significantly from that measured in plasma (wall-to-plasma ¹⁸F-DG concentration ratio = 0.9 ± 0.1).

Histological examination of the excised symptomatic plaques from all the patients who had undergone imaging revealed heavy macrophage infiltration.

Carotid plaque autoradiography with tritiated deoxyglucose demonstrated uptake in macrophage-rich areas of plaques, predominately at the lipid core/fibrous cap border of the lesions. There was little or no uptake in other areas of the plaques (Figure 2). Control sections showed no development of silver grains.

Discussion

Anecdotal reports of "hot spots" in blood vessels of patients at high risk of atherosclerosis undergoing whole body ¹⁸F-DG-PET studies, along with a single study in cholesterol-fed rabbits,⁸ have suggested that ¹⁸F-DG can accumulate in atherosclerotic plaques.

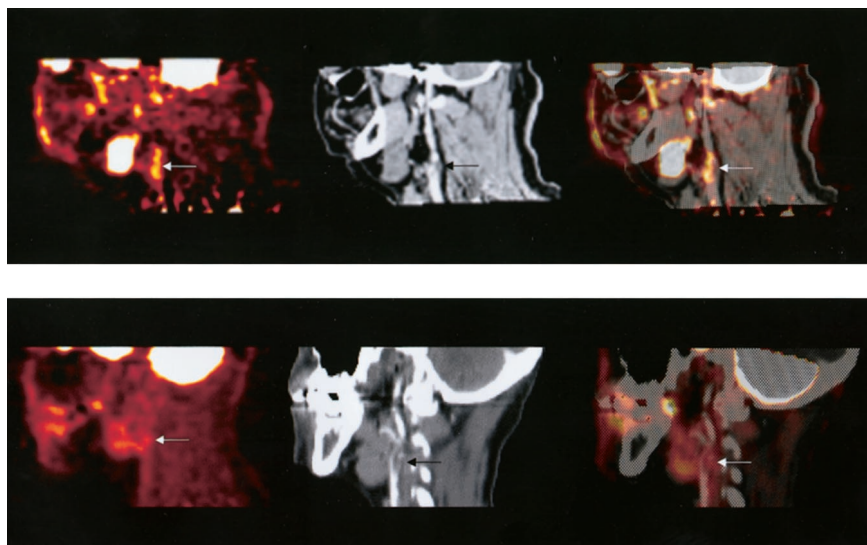


Figure 1. The upper row (from left to right) shows PET, contrast CT, and co-registered PET/CT images in the sagittal plane, from a 63-year-old man who had experienced 2 episodes of left-sided hemiparesis. Angiography demonstrated stenosis of the proximal right internal carotid artery; this was confirmed on the CT image (black arrow). The white arrows show ^{18}F FDG uptake at the level of the plaque in the carotid artery. As expected, there was high ^{18}F FDG uptake in the brain, jaw muscles, and facial soft tissues. The lower row (from left to right) demonstrates a low level of ^{18}F FDG uptake in an asymptomatic carotid stenosis. The black arrow highlights the stenosis on the CT angiogram, and the white arrows demonstrate minimal ^{18}F FDG accumulation at this site on the ^{18}F FDG-PET and co-registered PET/CT images.

By combining PET and CT imaging, we have confirmed that ^{18}F FDG accumulates in human carotid artery atherosclerotic plaques, with significantly higher uptake in symptomatic lesions than in asymptomatic lesions. Furthermore, we have demonstrated that the majority of deoxyglucose accumulates in macrophage-rich areas of the plaque. These findings suggest that inflammation is present to a greater degree in symptomatic plaques than asymptomatic plaques.

Taken together, these results suggest strongly that ^{18}F FDG-PET may be capable of imaging and potentially quantifying plaque inflammation. This raises the possibility that ^{18}F FDG-PET could be used to predict the risk of future plaque rupture, and therefore to target surgery to high-risk carotid stenoses regardless of angiographic appearance. Perhaps more importantly, it might be used to monitor the effectiveness of systemic atheroma-modifying treatments because it is likely that any measurable effects of treatment on inflammation in carotid atheroma will reflect similar changes in other vascular beds, including the coronary arteries.⁹

Before this potential can be realized, further studies are required to determine the precise relationship between ^{18}F FDG uptake, plaque macrophage activity, and risk of plaque rupture, and more macrophage-specific PET ligands will be required to image vessels in metabolically active tissues such

as the heart and brain. Although PET has limited spatial resolution (≈ 5 mm FWHM for GE Advance), we have demonstrated that co-registration with CT can localize the ^{18}F FDG signal to individual atherosclerotic lesions. Because CT angiography cannot accurately measure plaque volume (because remodeling can accommodate large plaques with little impact on lumen diameter), however, we were unable to apply partial volume correction to our data in this study. We are confident, however, that this will be achievable with high-resolution carotid MRI.¹⁰

In summary, this early study provides the first direct evidence that human atherosclerotic plaque inflammation can be assessed non-invasively by ^{18}F FDG-PET, and paves the way for a new approach to atheroma imaging that reflects the cellular pathology of the disease process rather than its anatomical consequences.

Acknowledgments

This work was funded by the British Heart Foundation and an Office of Science and Technology Technology Foresight Challenge Award. Professor Weissberg holds a British Heart Foundation Professorship. Dr Warburton is supported by a Private Patients Plan Mid-Career Fellowship. We are grateful to the staff of the Wolfson Brain Imaging Center, Addenbrookes Neuro-CT scanner, and the Depart-

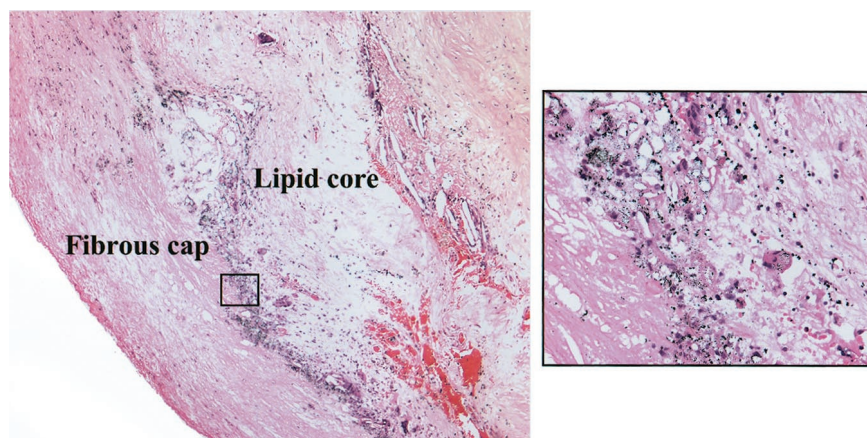


Figure 2. Tritiated deoxyglucose autoradiography of symptomatic carotid artery plaque. The larger panel shows typical plaque architecture, whereas the inset shows that silver grains have accumulated at the lipid core/fibrous cap border region, predominately within macrophages. Magnification $\times 10$ and $\times 20$.

ment of Pathology at Papworth Hospital for their kind assistance with this project.

References

1. Ross R. Atherosclerosis: an inflammatory disease. *N Engl J Med.* 1999; 340:115–126.
2. Davies MJ. Stability and instability: two faces of coronary atherosclerosis. The Paul Dudley White Lecture 1995. *Circulation* 1996;94:2013–2020.
3. Fishbein MC, Siegel RJ. How big are coronary atherosclerotic plaques that rupture? *Circulation* 1996;94:2662–2666.
4. Crisby M, Nordin-Fredriksson G, Shah PK, et al. Pravastatin treatment increases collagen content and decreases lipid content, inflammation, metalloproteinases, and cell death in human carotid plaques: implications for plaque stabilization. *Circulation.* 2001;103:926–933.
5. Sugawara Y, Braun DK, Kison PV, et al. Rapid detection of human infections with fluorine-18 fluorodeoxyglucose and positron emission tomography: preliminary results. *Eur J Nucl Med.* 1998;25:1238–1243.
6. Kinahan PE, Rogers JG. Analytic 3D image reconstruction using all detected events. *IEEE Trans Nucl Sci.* 1989;36:964–968.
7. Robb RA, Hanson DP. A software system for interactive and quantitative visualization of multidimensional biomedical images. *Australas Phys Eng Sci Med.* 1991;14:9–30.
8. Lederman RJ, Raylman RR, Fisher SJ, et al. Detection of atherosclerosis using a novel positron-sensitive probe and 18-fluorodeoxyglucose (FDG). *Nucl Med Commun.* 2001;22:747–753.
9. Hulthe J, Wikstrand J, Emanuelsson H, et al. Atherosclerotic changes in the carotid artery bulb as measured by B-mode ultrasound are associated with the extent of coronary atherosclerosis. *Stroke.* 1997;28:1189–1194.
10. Meltzer CC, Kinahan PE, Greer PJ, et al. Comparative evaluation of MR-based partial-volume correction schemes for PET. *J Nucl Med.* 1999;40:2053–2065.